Ocean Engineering 298 (2024) 117266

Contents lists available at ScienceDirect

Ocean Engineering

journal homepage: www.elsevier.com/locate/oceaneng

Comparative analysis of load reduction device stiffness curves for floating offshore wind moorings

Oscar Festa [a,*], Susan Gourvenec [a], Adam Sobey [a,b]

[a] Faculty of Engineering and Physical Sciences, University of Southampton, Southampton, SO16 7QF, UK
[b] Data-Centric Engineering, The Alan Turing Institute, London, NW1 2DB, UK

ARTICLE INFO

Keywords:
Load reduction devices
Floating wind turbines
Compliant moorings
Mooring system design
Taut moorings

ABSTRACT

Traditional mooring systems can be unsuitable and uneconomical for floating offshore wind turbines. Load reduction devices, which are extensible components installed along mooring lines, have been shown to reduce loads on anchors and mooring lines. This enables the use of smaller and lighter anchors and mooring components and reduces fatigue damage on the mooring system. Load reduction devices come in various forms, including ballasted pendulums, polymer springs, and hydraulic dampers, each with unique non-linear stiffness curves. These non-linear curves typically consist of either a progressively-increasing 'single-phase' stiffness, or a 'three-phase' stiffness which exhibit stiff first and third-phase responses with a low-stiffness second phase. Selecting the correct shape of stiffness curve is key to ensure optimal load reduction performance from the device. This study compares the impact of 4 different non-linear stiffness curves, including 2 single-phase curves and 2 three-phase curves, on tension reduction and platform motions through finite element modelling. Taut and catenary mooring configurations, in both shallow (75 m) and intermediate (150 m) water depths, during 50-year parked and 50-year operational load cases are considered. The IEA 15 MW reference turbine, on the reference Voluturn-US semi-submersible platform are adopted for the analyses. Of the 4 non-linear stiffness curves considered, those with three-phase stiffness offer the maximum load reduction compared to a base mooring with no load reduction device, and are most effective in reducing fatigue damage. All load reduction device stiffness curve types have little effect on out-of-plane motions of the platform and acceleration at the nacelle, but lead to an increase in horizontal offset, or surge, of the floating offshore wind turbine when compared to the base mooring system. The increase in surge is similar regardless of the load reduction device stiffness curve shape, and is shown to be mainly driven by the length and rated tension of the device.

1. Introduction

1.1. Motivation

Up to 80% of worldwide offshore wind resources are located in water depths greater than 60 m (WindEurope, 2017), where traditional fixed-bottom wind turbines become less economically viable. In these water depths, offshore wind turbines must be deployed on floating structures, which are connected to the seabed via mooring systems composed of mooring lines and anchors. Current floating offshore wind turbine (FOWT) mooring system designs are derived from decades of oil and gas practices, and typically employ heavy steel components (Ma et al., 2021) which are expensive and carbon-intensive to manufacture, transport and install. As FOWT farms require large numbers of structures to be moored to the seabed, reducing mooring system material costs per unit has the potential to provide significant reductions to the overall cost of a FOWT project, reducing the carbon footprint and capacity pressures of its supply chain.

The material cost of a mooring system is typically driven by the minimum breaking load (MBL) of mooring line components and the maximum holding capacity of the anchor, both of which must be designed to withstand the extreme loading experienced over the system's lifetime. A typical approach to reducing loads on a mooring system involves increasing the compliance of the mooring system, i.e., reducing its stiffness (Ma et al., 2019). All spread mooring systems exhibit some form of compliance, which can be either geometric or elastic. Geometric compliance describes the ability of the mooring to change shape under loading, e.g. a catenary mooring line lifting off the seabed, while elastic compliance determines the capacity of the mooring line to extend axially, e.g. elastic stretch of a section of polymer rope. By

* Corresponding author.
E-mail address: ogf1n20@soton.ac.uk (O. Festa).

https://doi.org/10.1016/j.oceaneng.2024.117266
Received 22 September 2023; Received in revised form 12 February 2024; Accepted 21 February 2024
Available online 28 February 2024

maximising the compliance of the system to fit the displacement criteria (primarily governed by the allowable range of the electrical power cable), loads on the system can be reduced, thus enabling the safe usage of more cost-efficient anchors and mooring line components.

In deep waters, taut and catenary mooring systems are inherently compliant due to the length of suspended line, which provides more elastic or geometric compliance. However, a significant portion of European floating wind to the mid-century is forecast to be in relatively shallow water depths, i.e., 50–150 m, where designing compliant mooring systems is challenging. Catenary configurations require heavier lines to achieve a reasonable pretension in shallower waters, which, combined with the fact more line gets lifted off the seabed for a given offset, leads to excessively stiff mooring systems and large footprints (Xu et al., 2020). For taut configurations, which typically employ polymer ropes, shallower waters lead to shorter lines for the same inclination angle, which means less available extension of the polymer rope, i.e. elastic compliance. More extension can be obtained by using a line angle closer to horizontal, which increases the length of rope, however this leads to larger footprints and higher material costs.

Load reduction devices (LRDs) are a nascent technology which introduce customisable compliance into a mooring system, so that the mooring system stiffness is not constrained by its physical and geometric properties (e.g. weight of chain, angle of mooring line, MBL of rope). This 'targeted' compliance provides a solution to the challenge of achieving a compliant mooring system in shallower water depths, without resorting to excessively large seabed footprints. LRDs, typically located close to the fairlead, act as non-linear springs that can safely operate at high levels of extension, i.e., 50% of the length of component compared to 5%–10% for traditional polymer rope. The key design parameter of an LRD is its non-linear stiffness curve, which effectively governs the stiffness of the mooring system. The non-linear stiffness curve is highly customisable by LRD manufacturers to provide greatest possible tension reduction whilst adhering to platform motion criteria. The devices can be tailored to a specific project environment and can be incorporated into catenary or taut mooring lines. The effect of the shape of the LRD non-linear stiffness curve on tension reduction and platform motions has not yet been comprehensively assessed for FOWT applications, and is the object of this research.

1.2. Background on LRDs

Current LRD concepts include the Technology for Ideas Seaspring (TFI), Dublin Offshore LRD (DO), and Exeter Intelligent Mooring System (IMS). The TFI device (Fig. 1a) is formed of a compressive polymer spring, which provides a low-stiffness, regressive response up until the steel flanges meet and the device 'locks-out'. The DO device (Fig. 1b) is formed of a part-weighted, part-buoyant cylinder which rotates under axial load to provide extension, counteracted by the restoring moments created by the weighted and buoyant sections. The IMS device (Fig. 1c) is composed of a hollow braided rope containing a water-filled pressurised bladder which resists reduction in the rope's diameter. The adjustable bladder pressure means the stiffness response of the device can be tuned in operation. Existing research around these LRD technologies has been highly driven by physical testing, and all three have been shown to successfully withstand the offshore environment (Harrold et al., 2020; OffshoreWind.biz, 2021; Offshore-mag.com, 2021).

Although the exact non-linear stiffness responses are customisable, each LRD concept has a characteristic curve shape, shown in Fig. 1, with two different curves chosen to represent different stiffness profiles achievable with the IMS device. Overall, the curves can be divided into two categories: '3-phase' curves (TFI, DO), or 'single-phase' curves (IMS 1, IMS 2). 3-phase curves have a high initial stiffness, then a low stiffness range over which the LRD is intended to operate, and a high third stage stiffness once compliance is exhausted. The single phase curves have a gradually increasing stiffness throughout.

Numerical modelling of the whole FOWT and mooring system is key at the design stage to ensure the optimal stiffness curve and length (or maximum extension) of the device are found for the specific application. Various studies, from the LRD developers, have provided such numerical modelling and assessed the performance of their LRD for a specific set of mooring and environmental input conditions. These studies provide little opportunity for comparison across LRDs, as variations in input conditions lead to vastly different results, ranging from 10% peak load reduction for the IMS (Harrold et al., 2020) to 59% reduction in peak load for the TFI (Lozon et al., 2022). Some further studies from the developers of the IMS have compared the performance of a specific LRD in different water depths, showing that tension reductions can be up to three times higher in 100 m water depth compared to 200 m (Khalid et al., 2020). Research by TFI developers has provided parametric analyses on LRD length, showing that longer LRDs provide increased tension reduction up to a certain point, with diminishing returns once sufficient compliance is reached (McEvoy and Johnston, 2019). The effect of various stiffness curve shapes for the TFI device has been compared (McEvoy and Kim, 2017), but this was for a tidal energy converter application rather than a FOWT. No existing study in the public domain has compared the stiffness curves for each of these devices, across constant sets of input conditions, for catenary and taut FOWT moorings. A summary of all numerical studies on LRDs for FOWTs, wave energy converters (WECs), and tidal energy converters (TECs) is given in Table 1.

1.3. Comparative analysis workflow

This paper presents a comparative analysis on the effect of different non-linear LRD stiffness curve shapes, each representative of a specific LRD concept, on tension reduction and platform motions for FOWT. To provide a comprehensive assessment with a broad range of applicability, the LRD stiffness curves were considered across a matrix of 8 different mooring scenarios and load cases:

- 4 mooring scenarios: 150 m depth catenary, 150 m depth taut, 75 m depth catenary, 75 m depth taut
- 2 load cases: parked 50-year extreme, operational 50-year extreme

The results were obtained from numerical modelling on a reference 15 MW wind turbine and semi-submersible platform. The model, mooring system, LRD modelling approach and load cases are described in the methodology. The results are then divided into three sections. The first two sections consider a fixed LRD length, and study the effect of the LRD curve shape on fairlead tension reduction and FOWT motions respectively. The third section compares the effect of varying the LRD length on fairlead tension and platform motions, for different LRD curve shapes.

2. Methodology

2.1. FOWT model description

The numerical modelling of the floater, turbine and mooring system was performed using Flexcom, a commercial finite element (FE) software. Flexcom offers fully-coupled aero-hydro-servo modelling using

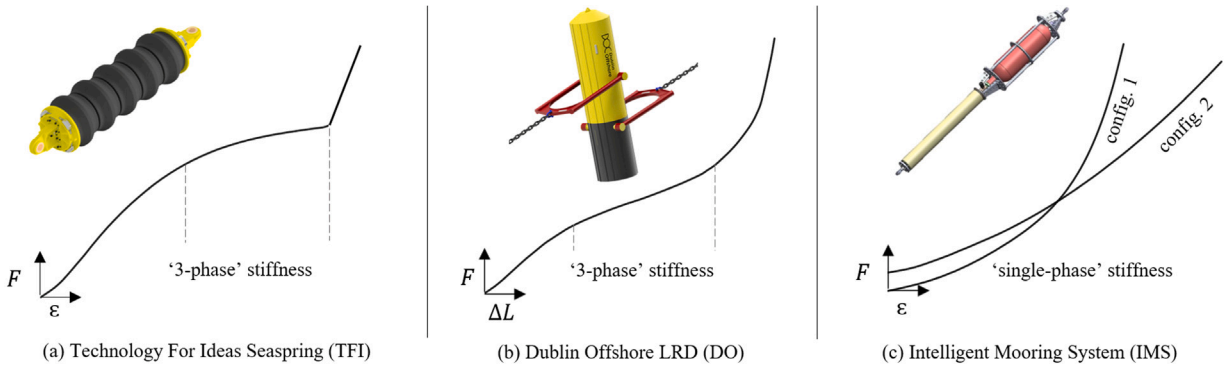

(a) Technology For Ideas Seaspring (TFI) (b) Dublin Offshore LRD (DO) (c) Intelligent Mooring System (IMS)

Fig. 1. Visualisation of the three different LRD concepts along with their characteristic stiffness curves: (a) Technology for Ideas Seaspring (TFI), (b) Dublin Offshore LRD (DO), (c) Intelligent Mooring System (IMS).

Table 1
Summary of publicly available numerical studies on LRDs, categorised by the parameterised variable(s).

Parameterised variable	Load case	Water depth	LRD length	Mooring configuration	LRD stiffness curve shape
Studies for WECs/TECs	Luxmoore et al. (2016)	Luxmoore et al. (2016)	McEvoy and Kim (2017)	Luxmoore et al. (2016)	McEvoy and Kim (2017)
Studies for FOWTs	Lozon et al. (2022), Khalid et al. (2020), Festa et al. (2022)	Khalid et al. (2020)	McEvoy and Johnston (2019), Harrold et al. (2020) Festa et al. (2022)	McEvoy et al. (2021), Pillai et al. (2022)	*no studies in public domain*

FAST plug-ins INFLOWWIND, AERODYN and SERVODYN, and has been validated against other commercial and academic software for a 5 MW turbine as part of an offshore code collaboration project (Robertson et al., 2020). The FOWT model used in this study is composed of the International Energy Agency (IEA) reference 15 MW wind turbine on the Volturn-US semi-submersible floating platform, and has been validated against the FAST model in Flexcom documentation (FLEXCOM, 2022). The full platform and turbine characteristics are described in detail in publications from the National Renewable Energy Laboratory (NREL) (Gaertner et al., 2020; Allen et al., 2020).

2.2. Base mooring description

Two conventional symmetric mooring configurations were studied, both composed of three evenly-spaced lines: a full-chain catenary mooring and a taut mooring composed of polyester rope with chain ends. Each mooring configuration was modelled in two water depths, 75 m and 150 m, resulting in a total of 4 mooring scenarios. Each scenario is shown in Fig. 2, annotated with the direction of wind and wave loading. All mooring components for both configurations (i.e. chain, polyester, and chain links) were given the same MBL of 15 MN for consistency in the comparative analysis. This corresponds to an R3 Studlink chain with a diameter of 143 mm, and Brydon–Bekaert MoorLine polyester rope diameter of 234 mm (Brydon, 2022). Pretension was also kept constant across all configurations and water depths, at 12.5% of MBL. The taut mooring was set at an inclined angle of 35 degrees with respect to horizontal, for both the shallow and intermediate water depth moorings, based on a previous study for taut FOWT systems (Bach-Gansmo et al., 2020). The mooring parameters are summarised for both mooring configurations in Table 2.

2.3. LRD modelling

To model the LRD mooring systems, the base mooring configurations were modified by substituting a non-linear spring element, representing the LRD, for a section of the line at each fairlead. No damping was attributed to the LRDs, aside from the mass damping of the whole mooring line included in the base Volturn-US Flexcom model (which was calibrated with the NREL model). This approach is in keeping with the numerical modelling from the various studies listed in Table 1. As the aim of this study is to compare different non-linear stiffness curves rather than the physical LRDs designs, physical properties such as diameter, linear mass and LRD length were equalised to provide a meaningful comparison. In practice, these parameters vary depending on the LRD concept considered, but also on the desired stiffness curve of the LRD. For the two spring-like devices, values of diameter and dry linear mass ranging from 0.3 m and 71 kg/m for IMS (Khalid et al., 2020), to 1.43 m and 1759 kg/m for TFI (Lozon et al., 2022) have been quoted in literature. The diameter of the cylindrical DO device, Fig. 1(b), typically ranges from 2.9–5.1 m, and the buoyant section is designed such that the full device is neutrally buoyant in water (Dublin Offshore, 2020). For this study, the LRD spring sections were all given a diameter of 1 m, and the dry linear mass was then set to 785 kg/m for neutral buoyancy in seawater. The lengths of LRDs considered also vary across different studies, ranging from 4 m (Harrold et al., 2020) to 30 m (McEvoy and Johnston, 2019). A length of 20 m was taken as the reference length for the LRD spring sections in this study, with subsequent comparison of additional lengths from 10 m to 30 m. By using standardised physical properties for all LRD concepts, the impact of the LRD stiffness curve on the system was isolated, which is key for this study. For more advanced studies on a specific LRD, a detailed, geometrically accurate LRD model should be employed to capture additional hydrodynamic or mechanical characteristics.

Non-linear stiffness curves for each LRD concept were reproduced from developer documentation, and normalised such that all LRDs exhibit the same tension at 0.5 strain (i.e. 10 m extension for the 20 m spring sections considered). For each of the 4 curve shapes, shown in Fig. 1 for the 3 devices, the stiffness is scaled depending on its 'rated tension', which is defined in this study as the tension in the device at 0.5 strain. DO and TFI refer to the rated tension as the 'Safe Working Load'

Table 2
Mooring parameters of the base mooring system. See Appendix for stiffness of the full mooring systems.

Mooring configuration	Taut inclined (35 deg)	Catenary
Pretension	1.875 MN	1.875 MN
Material type	Brydon Moorline Polyester	R3 Studlink Chain
MBL	15 MN	15 MN
Diameter	234 mm	143 mm
Stiffness (EA)	100 MN	3750 MN
Mooring radius (m)	252 (150 m depth); 145 (75 m depth)	640

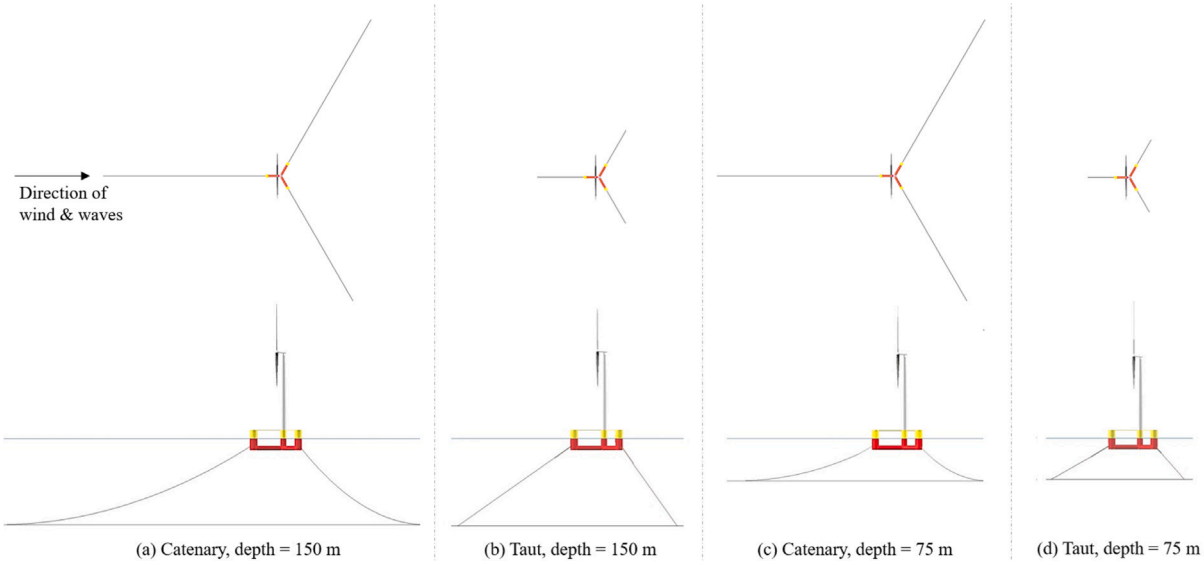

Fig. 2. Top-down and side views of the 3D Flexcom model of the IEA 15 MW wind turbine on the Volturn US platform, for the four mooring scenarios considered in this paper.

and 'Target Load' respectively. In practice, these different rated tensions are obtainable by changing the dimensions and/or material properties of the LRD. Higher rated tensions often apply to locations with more severe environmental loading, which typically require higher MBLs, but the LRD's MBL and rated tension are not inherently coupled. The MBL of the LRD can be can be adjusted to whichever value meets safety requirements, whereas the rated tension is a separate design variable which drives performance of the device. In this study, selected rated tensions range from 2.5 MN, which is just above the mooring pretension, to 7 MN, which is just below the maximum expected tension with no LRD, determined from an analysis on the base-case mooring system. The 10 rated tensions considered in this study are shown for each of the 4 stiffness curve shapes in Fig. 3. Each combination of LRD stiffness curve shape, rated tension and mooring scenario then leads to a different stiffness curve of the mooring system as a whole. Full mooring stiffness curves are shown for each combination in the Appendix.

2.4. Design load cases

The load cases applied in the model are representative of the New York Bight area (Lozon et al., 2022). Two load cases were considered: a 50-year return period load case for an operational wind turbine, and a 50-year return period load case for a parked turbine, i.e., with feathered blades to reduce wind loading. For the operational load case, the wind speed equals the turbine's rated wind speed of 10.59 m/s, generating the highest amount of wind thrust on the system (Gaertner et al., 2020). This scenario can sometimes cause higher tensions on the mooring system than more extreme conditions with a parked turbine, hence both load cases require consideration as potential design driving scenarios. The parameters of each load case are summarised in Table 3.

Table 3
Operational and parked load cases used in this study (Lozon et al., 2022).

Load case	50-yr operational	50-yr parked
IEC load case reference	IEC 1.6	IEC 6.1
Wind speed (m/s)	10.59	41.10
Turbulence intensity	0.085	0.154
Significant wave height (m)	4.72	8.70
Peak wave period (s)	10.03	12.73
Peak shape parameter	2.02	2.03
Current	not considered	not considered

The two load cases were run on all 4 base mooring scenarios for the IEC-recommended duration of 3600 s (International Electrotechnical Commission, 2019), with wind and waves acting in the direction shown in Fig. 2. For the irregular wind and wave seeds considered, the highest loads on the windward mooring line occurred in the first 1200 s of the simulation. The resulting time-series of fairlead tension and surge (i.e. horizontal platform offset), were cropped to the first 1200 s and are shown in Fig. 4.

The fairlead tensions are highest for the taut moorings in 75 m water depth (Fig. 4d), due to the lowest compliance in the mooring system. These high fairlead tensions, which are essentially restoring forces maintaining the platform in position, translate to much lower surge of the platform (see Fig. A.1 in Appendix for additional discussion). Conversely, the catenary mooring in 150 m depth (Fig. 4c), is the

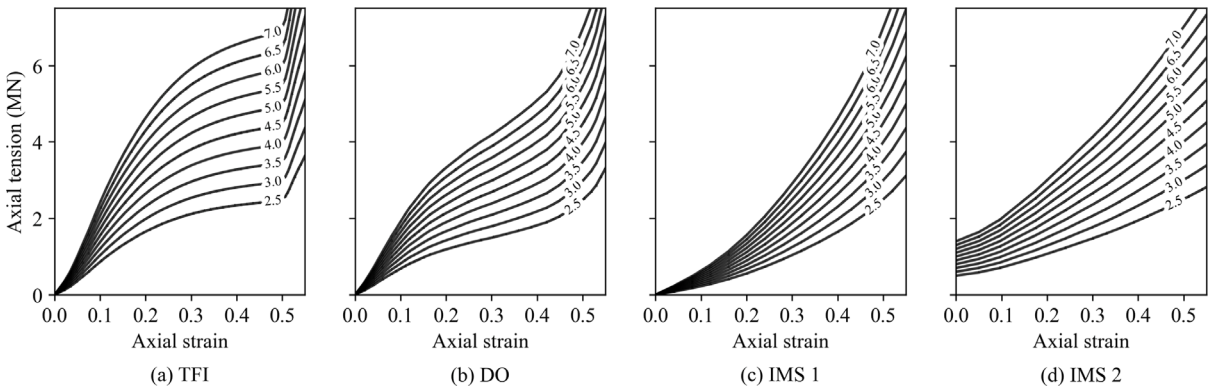

Fig. 3. : Tension–strain plots for the 4 non-linear curve shapes considered in the study, which are attributed to the spring elements representing the LRDs in the FE model. 10 different rated tensions are modelled for each curve shape, from 2.5 MN to 7 MN, which determine the tension at 0.5 strain (i.e., at 10 m extension for the 20 m spring length).

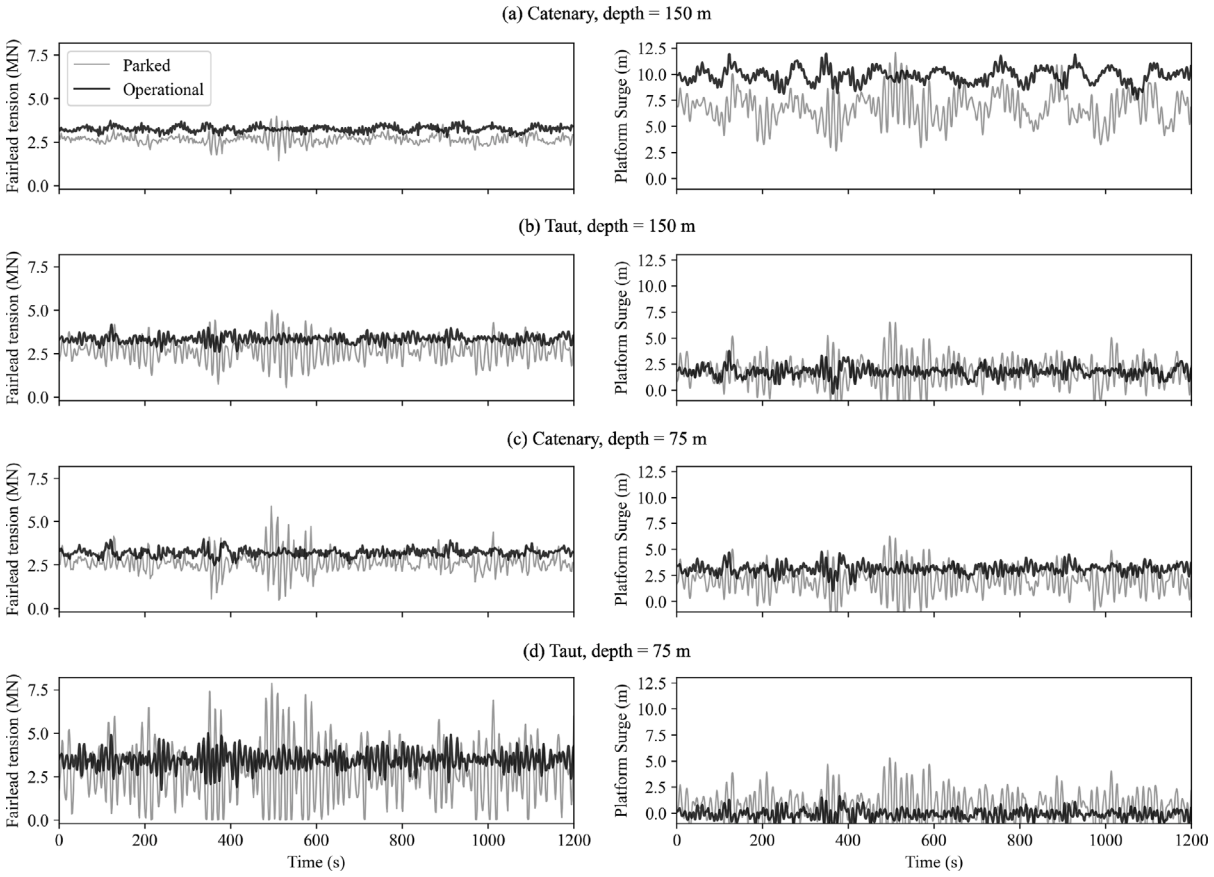

Fig. 4. Time-series of fairlead tensions and platform surge for the four base-case mooring scenarios, for parked and operational load cases.

most compliant and shows the highest surge and lowest tensions at the fairlead. Under the 50-year parked load case, the shallow taut configuration also exhibits numerous 'slack' events, where the fairlead tension momentarily reaches zero. These events can potentially be damaging to the mooring system. In practice, this mooring system would not be viable without an LRD for the given conditions, and a line angle much closer to horizontal would have to be considered to increase the line length and deliver more compliance. However, this steep line angle was maintained for the taut-line model as it provides two advantages for this study: 1. The taut-line angle is similar to the catenary line hang-off angle at the fairlead, leading to comparable ratios of vertical to horizontal forces across both configurations; 2. Less contribution of synthetic rope towards the compliance of the system puts more emphasis on the behaviour of the LRDs.

3. Effect of the LRD stiffness curves on tension reduction

3.1. Significance of the LRD rated tension in stiffness curve comparison

To compare the LRD stiffness curves, the loading time-series shown in Fig. 4 are applied to the LRD mooring system, for each of the 4 different stiffness curve shapes and 10 rated tensions shown in Fig. 3.

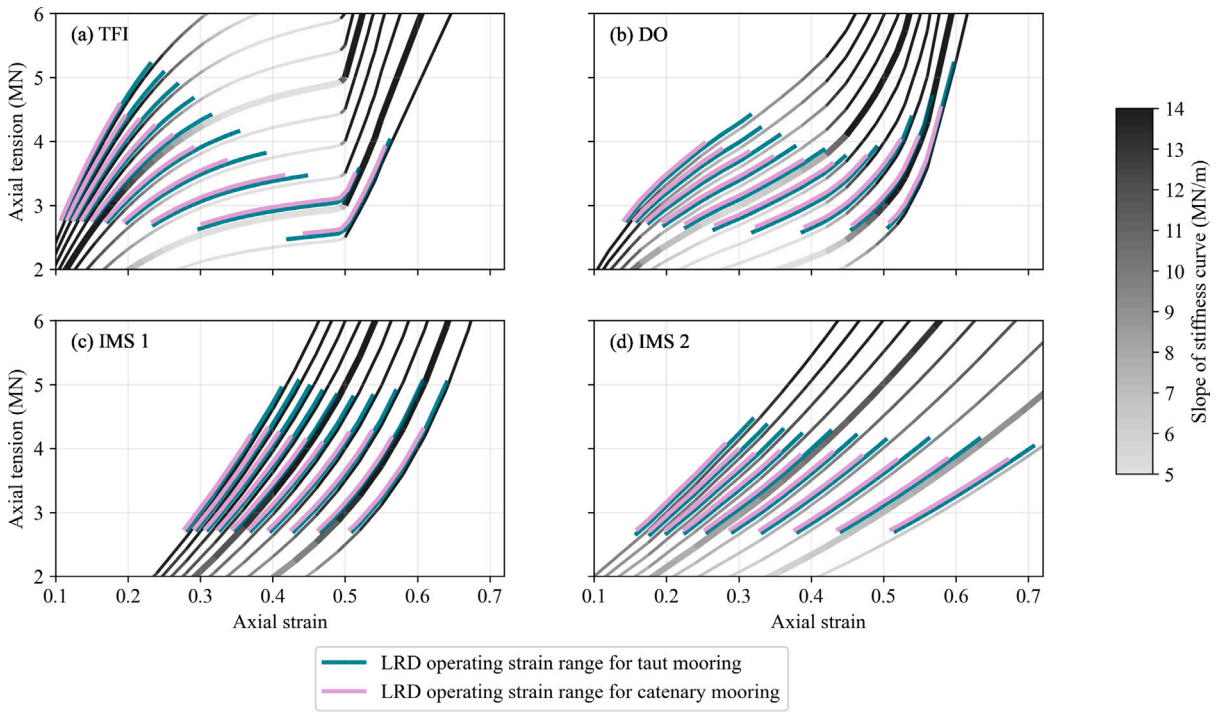

Fig. 5. Stiffness curves plotted for each rated tension and curve type, and colour graded according to the slope of the stiffness curve. The operating strain region of the LRD, for the 75 m water depth and parked load case, is plotted on top of each curve. The 3 MN and 5 MN rated tension curves are shown with thick lines.

For the 3-phase curves, the rated tension defines the point at which the LRD enters its third-phase stiffness. However, in a more general sense, the rated tension defines the overall steepness of the non-linear stiffness curve, i.e. its slope $dT/d\epsilon$. This impacts the performance of the LRD, by affecting the phase of the stiffness curve over which it operates and is effective in reducing tension. This is depicted in Fig. 5, which shows the span between the mean LRD strain and the maximum LRD strain over the course of the time-series, defined as the 'operating strain region'. For brevity, the operating strain regions are shown only for the highest load conditions, i.e. 75 m water depth and parked load case.

For all 4 stiffness curve shapes, the lower rated tensions lead the LRD to operate in higher strain regions. For the two single-phase curve shapes (Figs. 5c & 5d) this has limited significance, as the slope of the stiffness curve is similar regardless of the operating strain region. However, for the 3-phase curve shapes (Figs. 5a & 5b), the slope of the stiffness curves varies considerably depending on the operating strain region. The lowest maximum tensions, i.e. tension at maximum strain, are found when the LRD operates in the second phase stiffness, which has the lowest stiffness curve slope. Thus, to obtain the full benefit of the LRD in extreme 50-year conditions, the rated tension of 3-phase curves must be low enough for the LRD to stretch past its first-phase stiffness, but high enough such that it doesn't exceed its rated tension and operate in its stiff, third phase.

To visualise the effect of different LRD stiffness curve shapes and rated tensions on the system, Fig. 6 shows a time-series of fairlead tension for the LRD moorings plotted against the base-case mooring, for all 4 mooring scenarios in the parked load case. For each of the stiffness curve shapes, 2 rated tensions are considered, 3 MN and 5 MN. The time-series are cropped to capture the peak loading events, which occur between 450 s and 550 s in the parked load case, for the wind and wave seeds considered (see Fig. 4). For the conditions considered, all LRDs offer peak tension reduction, and eliminate slack line events in the taut mooring configurations. Greater tension reduction is apparent in mooring scenarios with less inherent compliance in the base-case mooring configuration, i.e. in the taut line and shallow water moorings (Fig. 6d).

As expected, LRDs with 3-phase stiffness curves, TFI and DO, show different fairlead tension responses depending on their rated tension, whereas the single-phase stiffness curve LRDs show similar responses for the two rated tensions considered. For the DO device, the 3 MN rated tension LRD is too soft, thus operating in the third phase stiffness and not reducing tension as much as the stiffer 5 MN LRD which operates in the second phase as intended. Conversely, the 5 MN TFI device is too stiff, thus operating in the first phase of its stiffness curve and not reducing tension as much as the 3 MN device. However, as shown by the operating strain region of the 3 MN TFI curve (Fig. 5a) the device momentarily exceeds its rated tension and enters its third phase stiffness at the maximum load for the 75 m water depth case. This is visible in the time-series of the TFI device (Fig. 6d, at 490 s and 510 s), where a secondary peak in tension appears, caused by the device 'locking-out' at 50% strain as it suddenly enters the high-stiffness third phase.

3.2. Maximum fairlead tension reduction

In the following results, the maximum fairlead tension reduction provided by different LRD curve shapes is compared across all rated tensions, to ensure the optimal rated tension is captured for each curve shape. Maximum fairlead tension is recorded over the full time-series for each LRD curve shape, and compared to the tensions in the base mooring for the same conditions (Fig. 7).

Across all 8 sets of input conditions, the 3-phase stiffness curves (TFI, DO) show better maximum tension reduction than the single-phase curves (IMS 1, IMS 2), as long as a suitable rated tension is selected. The window of suitable rated tensions, which allow the LRDs to operate in their second phase stiffness, is smaller for the TFI curve (3–4 MN) than for the DO curve (4–6.5 MN). This is due to the low, regressive slope of the TFI stiffness curve in its second phase (less

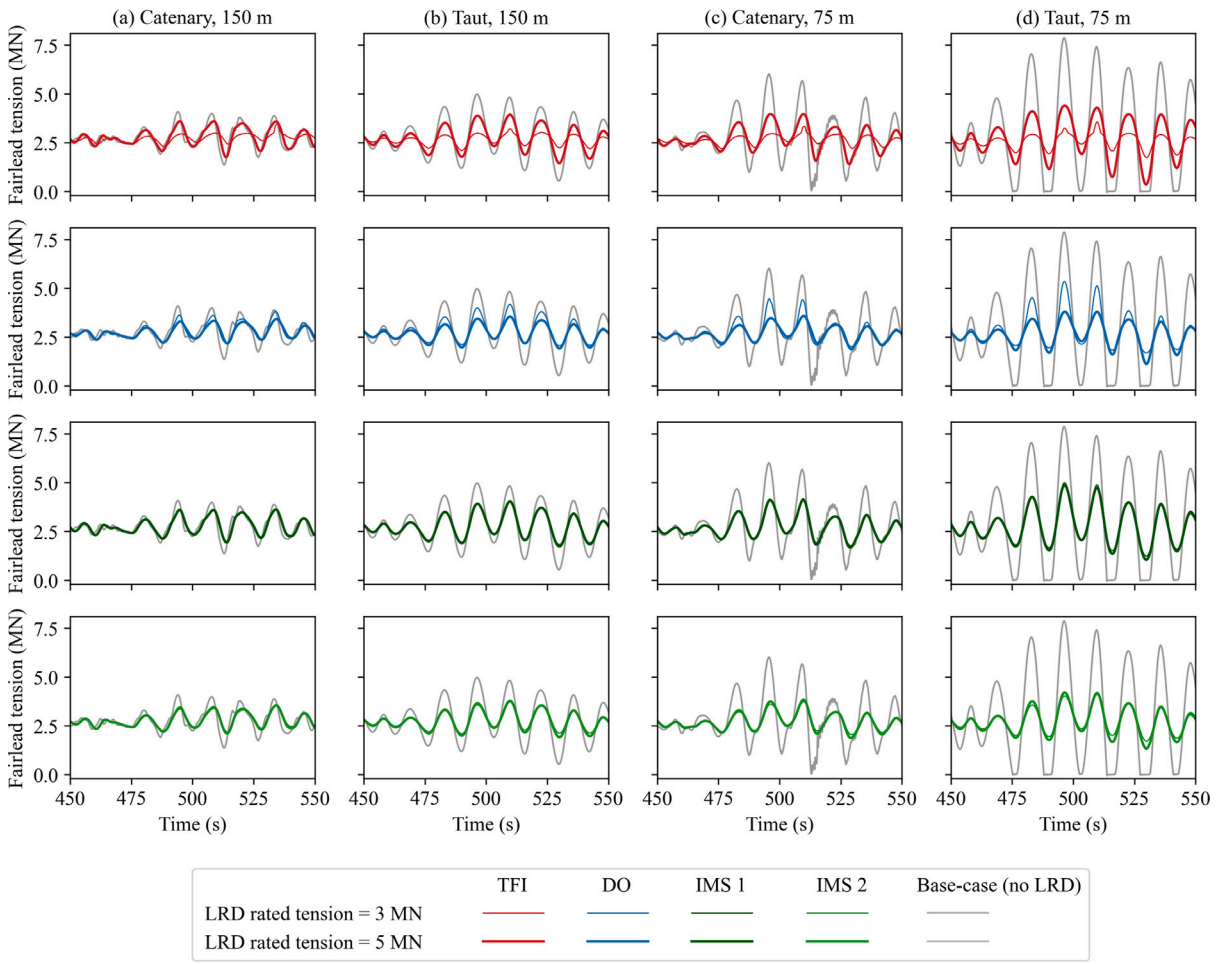

Fig. 6. Peak fairlead tension event in parked turbine load case. Time-series for each LRD is plotted against no LRD case, for two values of rated tension.

than 5 MN/m), which is highly effective at reducing tension, but also translates to rapid extension of the device the as it approaches its rated tension. The DO curve has a stiffer second-phase response, leading to slightly lower tension reduction, but enabling a greater range of rated tensions to operate within the second phase.

In the scenario where peak loads are design-driving, the rated tension which provides the highest tension reduction would theoretically be the most advantageous. However, in some cases, selecting this rated tension could lead to the LRD exhausting its compliance and exceeding its rated tension. For instance, with the TFI LRD in the taut 150 m case (Fig. 7b), a rated tension of 3 MN provides the highest tension reduction. However, the maximum fairlead tension when using this device is of 3.2 MN, meaning the LRD has exceeded its rated tension and entered its third-phase, 'lock-out' stiffness. If the 'optimal' rated tension for the specific application is defined as that which provides the highest tension reduction without the LRD exceeding its rated tension, a rated tension of 3.5 MN should be chosen for the TFI curve. Similarly, the 'optimal' rated tensions for this application would be taken as 4.5 MN for the IMS and DO LRDs.

In general, all curves offer better tension reduction in the parked load case than in the operational load case. This can be put down to two factors: 1. The higher waves in the parked case create more dynamic tension, which in turn increases the effectiveness of the LRDs (Festa et al., 2022); 2. the lower wind thrust in the parked case leads to a lower effective strain range in the LRD, meaning more compliance is left to reduce the peak wave-induced loading. The wind thrust in the operating case causes a constant, 'background' load, which displaces floater from its reference position, stiffening the mooring system in the process. This offset increases the mean strain of the LRD, meaning less compliance is available to reduce peak dynamic wave loads. This is especially apparent with lower rated tensions on the 3-phase curves, where the LRD has exhausted its compliance under the background load, leading to an increase in maximum tension.

3.3. Fatigue damage reduction

In addition to reducing the tension caused by the maximum loading event, which can lower the required material cost of a FOWT moorings and anchors, LRDs also reduce the tension on the mooring system caused by other, lesser, loading events. The damage caused by these lesser loads can accumulate over the structure's lifetime, causing fatigue in the mooring components which constitutes the leading cause of chain failure for permanent moorings (Fontaine et al., 2014). The reduction in lower-amplitude loads is apparent in the time-series shown in Fig. 6, where 'smaller' peaks in tension occurring at 450 s and 475 s are reduced by the LRDs. This tension reduction reduces the overall damage caused on the chains, ropes, and mooring components, which can extend their fatigue life and reduce the risk of failure. To portray this, the magnitude and timestamp of every fairlead tension peak were measured from the original time-series of the base-case moorings, for each of the time-series shown in Fig. 4. For each peak, the resulting tension reduction for the LRD moorings is measured and scattered

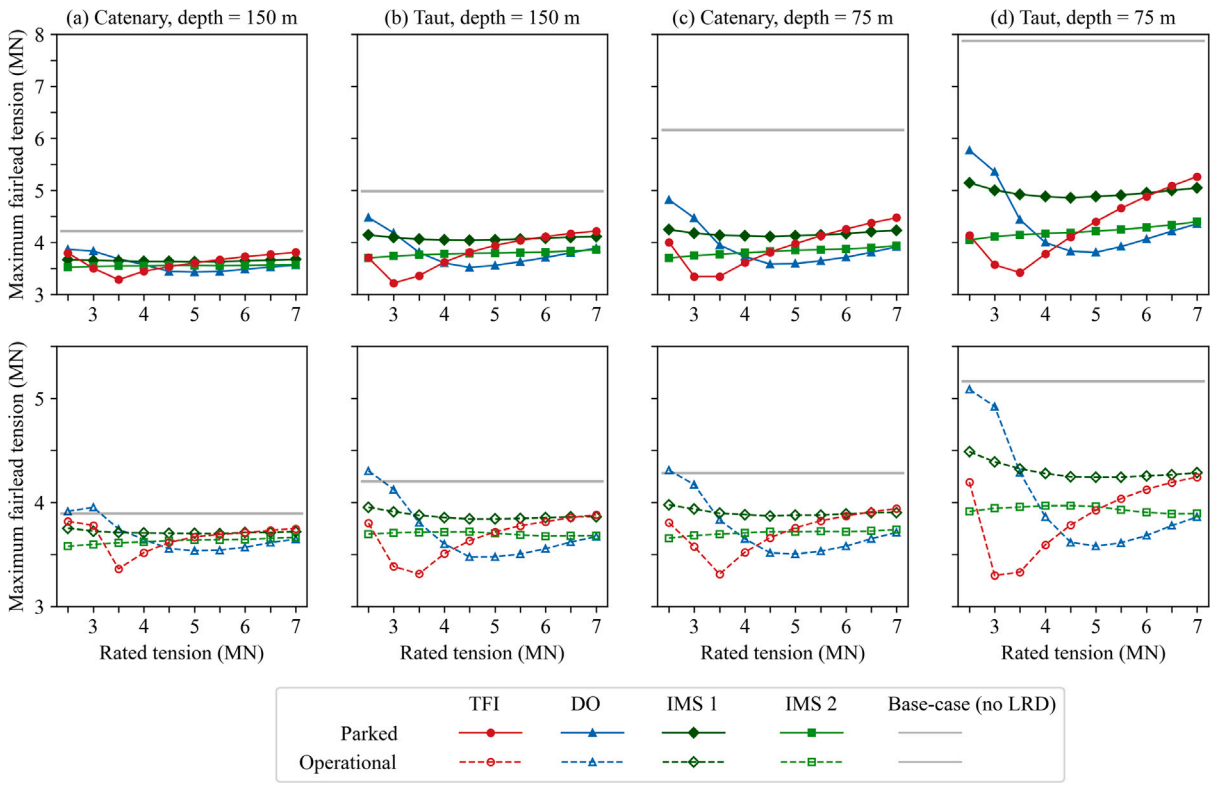

Fig. 7. Maximum fairlead tension for each of the 4 LRD curve types across a range of rated tensions. Each of the 8 subplots represents a same set of input conditions, covering all 4 mooring scenarios and 2 load cases.

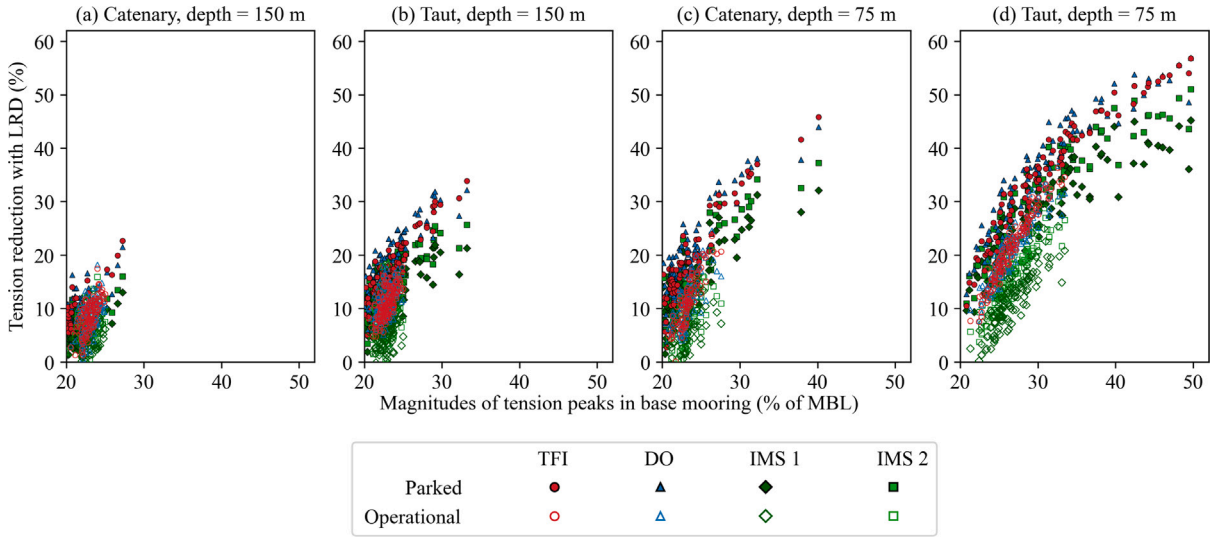

Fig. 8. Reduction in tension provided by each LRD (with rated tensions of 3.5 MN for TFI, and 4.5 MN for DO, IMS1, and IMS2) for individual fairlead tension peaks across the time series, plotted against magnitude of the peak in the base-case mooring scenario, i.e. without LRD.

against the magnitude of the original peaks (Fig. 8), using the optimal rated tensions determined in Section 3.2.

These results show a strong correlation between peak load magnitude in the base-case mooring, and the resulting tension reduction provided by the LRD. The moorings with more inherent compliance (Fig. 8 a & b) do not experience loads above 35% MBL, thus do not obtain the full benefit of the LRDs. Peak load reductions in the operational load case follows the same correlation, albeit with slightly lower reductions due to more of the LRD compliance being consumed by the background wind load. The 3-phase stiffness curves, TFI and DO, are shown to offer the best tension reduction across all load magnitudes above 20% MBL, regardless of the mooring scenario or load case, which suggests they provide the highest damage reduction.

The total fatigue damage caused over a specific duration can be estimated by a metric known as the damage equivalent load (DEL). For a given irregular loading time-series, the DEL represents the amplitude of a constant cyclic load that results in the same cumulative fatigue damage as the irregular loading time-series itself (ASTM International, 2011). This was calculated using a rainflow counting algorithm, with a fatigue slope of 5 (Lozon et al., 2022), for each full time-series. The

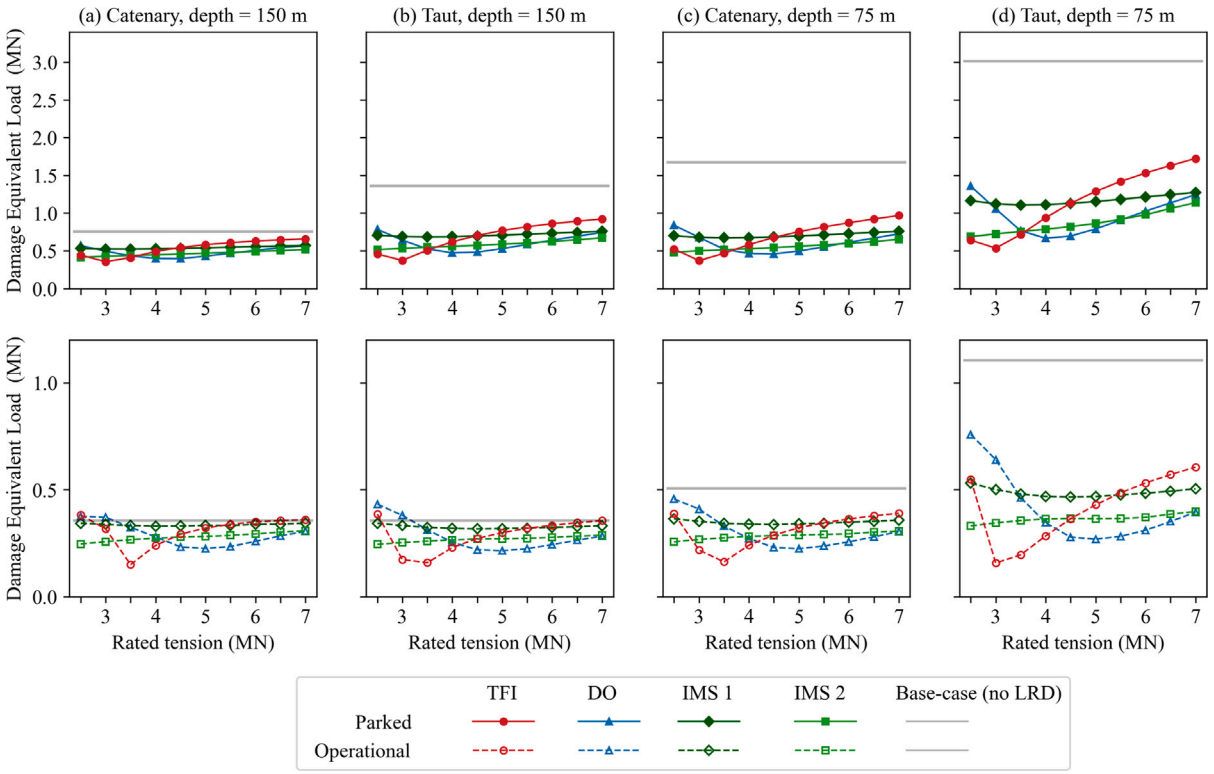

Fig. 9. Damage equivalent load over the full time-series for each of the 4 LRD curve types and 10 rated tensions considered. Each of the 8 subplots represents a same set of input conditions, covering all 4 mooring scenarios and 2 load cases.

resulting DEL is shown in Fig. 9 for each rated tension and stiffness curve type.

As with maximum load reduction, the DEL reduction is highest in the taut moorings and shallower waters, where there is less inherent compliance in the base-case mooring system. The effect of the LRD stiffness curve shape on the DEL follows a similar pattern to its effect on the maximum tension, with the three-stage stiffness curves offering the most DEL reduction, as long as suitable rated tensions are selected. However, the rated tensions which provide highest DEL reduction are slightly lower than the rated tensions which provide highest maximum load reduction, as the lower stiffness can better reduce the impact of lesser loads. In the taut 75 m case for instance (Fig. 9d), the 3 MN TFI and 4 MN DO curves provide highest DEL reduction, whereas the 3.5 MN and 4.5–5 MN curves provide highest maximum load reduction (see Fig. 7d). In the scenario where fatigue is design driving, the lower rated tension could be considered, at the cost of the device potentially exceeding its rated tension and entering its third phase stiffness under the maximum load. Whether this trade-off is acceptable would depend on the type of LRD and developer guidance.

4. Effect of LRD stiffness curves on platform motions

4.1. Significance of platform motions

In the offshore environment, the FOWT platform exhibits motions in 6 degrees of freedom (DOFs), as depicted in Fig. 10. When altering the stiffness response of a mooring system, such as by introducing an LRD, it is crucial to consider the subsequent impact on the motions of the platform. Since the wind and wave loads considered in this study are acting along the same axis (surge axis in Fig. 10), only the DOFs in the plane parallel to this axis are considered, i.e. only the surge, pitch and heave DOFs. FOWT projects typically have strict

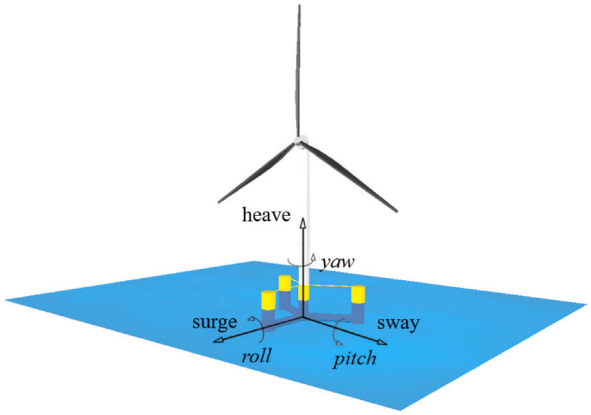

Fig. 10. Visualisation of the 6 DOFs of the FOWT platform. Rotational motions are shown in italics.

criteria regarding the maximum allowable motions in these 3 DOFs, as they can cause undesirable effects to the system: surge (i.e. horizontal platform offset) can damage the power cable if its allowable range is exceeded; pitch affects the efficiency of energy production; and high nacelle accelerations can cause structural and mechanical damage to turbine components (Taboada et al., 2020).

Mooring designs for FOWTs must allow the system to safely operate within the maximum motion criteria. This is particularly important for surge, as the maximum surge under a given set of environmental loads is directly dependent on the stiffness of the mooring system (see Appendix). Motions and accelerations outside of the water plane such as heave and pitch are typically more influenced by the hydrodynamics of the platform than by the mooring system, but must be considered in mooring design nonetheless. This section studies the effect of LRD

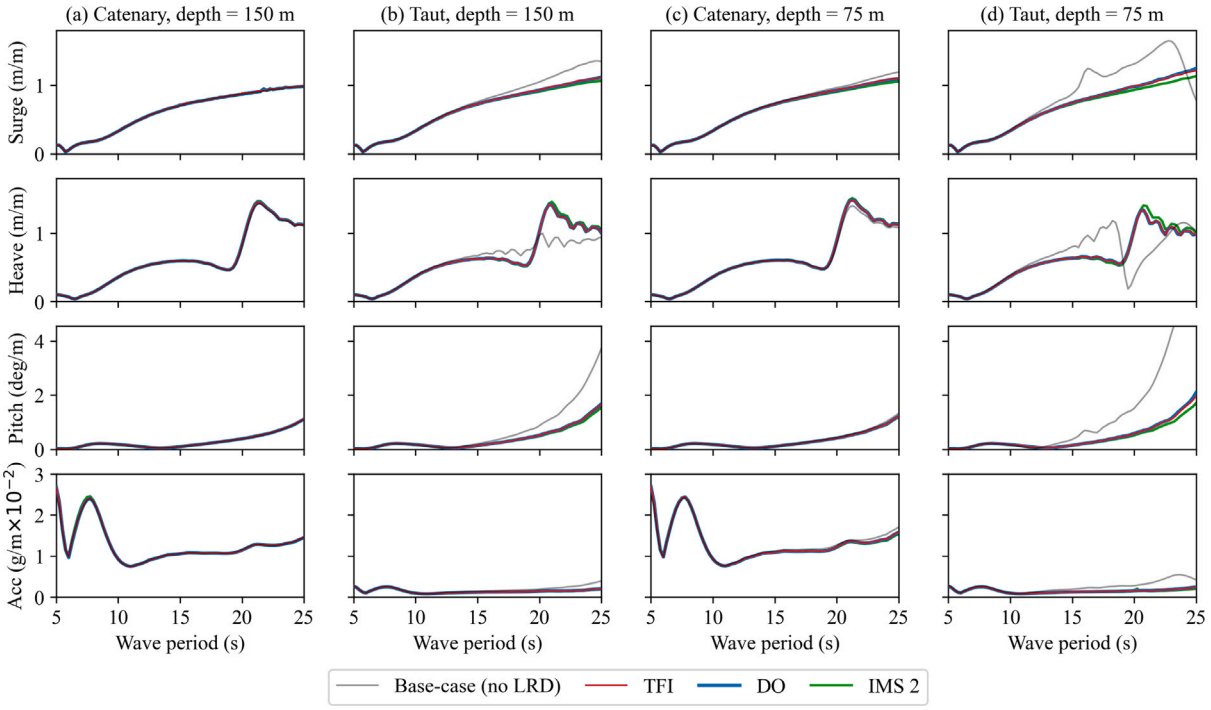

Fig. 11. Effect of regular wave-only loading on platform surge, heave, pitch and nacelle accelerations.

stiffness curves on platform motions and nacelle accelerations. For brevity, IMS 1 is omitted, and one rated tension is selected for the 3 other LRDs, which correspond to the 'optimal' rated tensions described in Section 3.2: 3.5 MN for TFI and 4.5 MN for DO and IMS 2.

4.2. Wave-induced motions

To isolate the effect of the LRDs on wave-induced motions of the structure, wind loading was disabled, and the full FOWT and mooring system were subjected to a set of regular Airy waves with varying frequency and fixed amplitude of 2.36 m. The amplitude of motion was measured, normalised with respect to the wave amplitude, and plotted against the frequency of the waves. The resulting statistic forms the Response Amplitude Operator (RAO). RAOs for the 4 key motions are shown in Fig. 11, for each mooring scenario and LRD stiffness curve type.

For the catenary configurations, the RAOs of the LRD moorings are near identical to those of the base moorings. This is in agreement with the full mooring system stiffness curves shown in Appendix, which suggest that at low offset, the base moorings and LRD moorings have the same stiffness (i.e., same gradient of tension–offset curve). This is not the case for the taut moorings, which are much stiffer without the LRD, and hence highly sensitive to the introduction of an LRD, leading to a more visible effect of the LRD on the RAO curve.

These results show that the addition of the LRDs does not introduce problematic frequencies for wave-induced motions, irrespective of the LRD stiffness curve shape. In fact, for the taut moorings, surge, heave and pitch motions are slightly reduced across key wave periods, 10–15 s. This reduction is higher in the shallow water scenario. Heave response is increased by LRDs at very high wave periods, 20–25 s, but these are typically not experienced in realistic sea states so should not be of concern.

4.3. Wind-induced motions

To isolate the effect of the LRDs on wind-induced motions of the structure, the full FOWT and mooring system were subjected to the same irregular wind conditions used in Section 2.4, but without waves. Resulting time-series of surge (i.e. horizontal platform offset), heave, and horizontal nacelle accelerations are shown in Fig. 12, cropped to show the peak loading event, which occurs at different timestamps for the parked and operational cases. Only 75 m water depth mooring scenarios are displayed, as these are most sensitive to LRDs as shown in Fig. 11. The vertical degrees of freedom (heave, vertical acceleration) are omitted as the absence of waves means loading is purely horizontal.

The wind generates a constant 'background' load on the structure, especially in the operational case where the thrust on the turbine is at its highest. The subsequent moment on the turbine also leads to high mean pitch (Fig. 12 c & d). During the parked case (Fig. 12 a & b), the blades are feathered to shed load, but the wind speed is much higher (41.10 m/s vs. 10.59 m/s for operational) and less regular, leading to a more varying response for both surge and pitch. In both parked and operational cases, the negligible dynamic loading means nacelle accelerations are low.

In both cases, with the absence of waves, the relationship between fairlead tension and platform surge is essentially quasi-static: the platform finds an equilibrium position, which is determined by the stiffness of the mooring system. Hence, the presence of an LRD, which reduces the mooring stiffness, increases the mean surge (or horizontal offset) of the platform. However, the mean pitch, which is mostly influenced by platform design rather than mooring stiffness, is not increased by the LRD. Overall, when similar rated tensions are considered, these trends do not depend on the shape of the LRD stiffness curve.

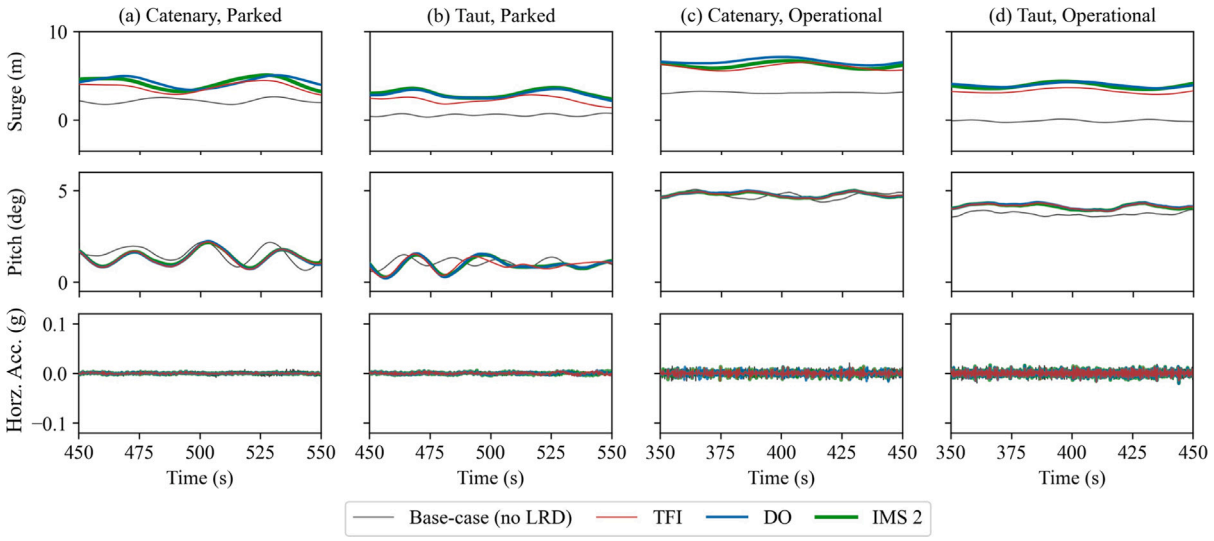

Fig. 12. Effect of wind-only loading on platform surge, pitch and horizontal nacelle accelerations, for 75 m water depth.

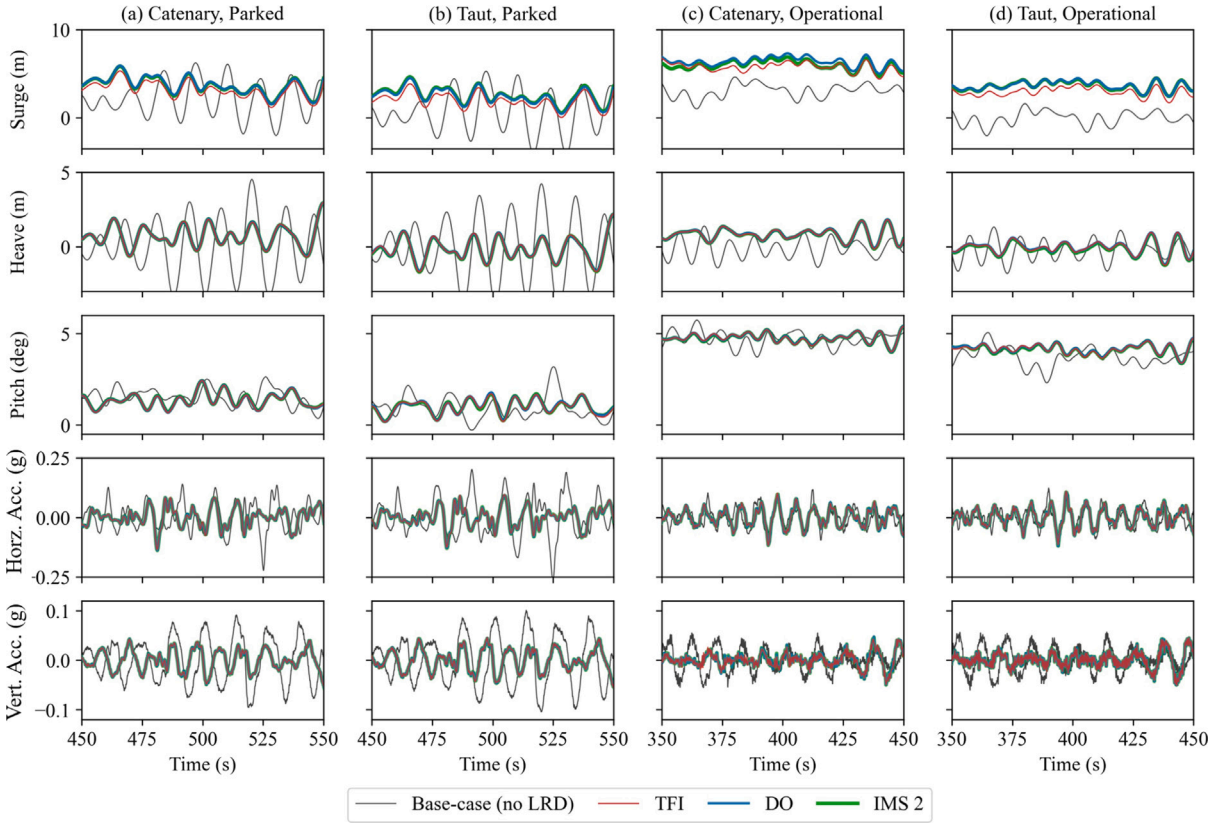

Fig. 13. Effect of combined wind and waves on platform motions in 3 DOF and nacelle accelerations in 2 DOF (vertical and horizontal), for 75 m water depths.

4.4. Combined wind and wave motions

Having studied the effect of LRDs on the motion response to wind and wave loading individually, the next step is to analyse the response to combined wind and wave loading. The same design load cases as described in Section 2.4 are considered, and time-series of the relevant platform motions in the wind/wave plane are recorded for each LRD curve type. Resulting time-series of platform motions are shown in Fig. 13, cropped to show the peak event. For brevity, only the 75 m water depth mooring scenarios are displayed, as these are the most sensitive to LRDs.

The general effect of the LRDs on platform motions and nacelle accelerations, regardless of stiffness curve shape, can be summarised as follows:

- Although the wind-induced surge component is increased by LRDs (as shown in Section 4.3), the damping effect from the LRDs results in a lower wave-induced dynamic surge response. This leads to a higher increase in surge in the operational case with higher wind loading (Fig. 13 b and c) than in the parked case with

higher wave loading (Fig. 13 a and b). Thus, the governing design case, i.e. case of maximum surge, can become the operational case when incorporating an LRD.
- Heave motions caused by the lower frequency waves, occurring at 500 s in the parked condition, are reduced by the LRDs, which is consistent with the RAO results. As the heave motion is driven by wave height, amplitudes are higher in parked condition with a higher significant wave height.
- Pitch oscillations are due to wave loads, whereas the mean pitch is caused by the moment from the wind thrust on the rotor, leading to much higher mean pitch in the operational load cases compared to the parked load cases. The wave-induced pitch oscillations are reduced by the LRDs, but the mean pitch is not affected, as was shown in Section 4.3.
- Wave-induced accelerations at the nacelle are reduced by LRDs for both the horizontal and vertical components, especially in the parked load case.

Overall, as was shown in the RAOs, the variation in stiffness curve shape of an LRD has very little effect on the motion response of the platform when compared to the response with the base-case mooring, i.e. without the LRD. All LRD curve shapes reduce oscillatory motions for pitch, heave and nacelle accelerations, but increase maximum surge (i.e. horizontal platform offset) of the platform. The surge motion is the only case where slight differences could be noted between the three LRD curve shapes. This is due to differences in the extension of the LRDs, which are minimal as the rated tensions considered across the 3 devices (3.5 MN, 4.5 MN, 4.5 MN) were similar.

5. Sensitivity analysis of LRD length

5.1. Significance of LRD length in stiffness curve comparison

Previous analyses in this paper have considered two LRD design parameters: stiffness curve shape and rated tension. Another key design parameter is the maximum extension of the LRD, which is defined by the length of the LRD section in the FE model. This determines the amount of compliance introduced by the LRD, and can make a significant difference to the overall tension–offset profile of the mooring system (Festa et al., 2023). The LRD length has been fixed at 20 m in the results presented so far, i.e., a maximum extension of 10 m when the LRD reaches its rated tension at 50% strain. In practice, the 'length' of the LRD section, or its maximum extension, would be increased by combining multiple devices in series, or in the case of the mechanical DO device, by increasing the distance between its hinge points.

5.2. Influence of LRD length on tension reduction

Fig. 14 shows the effect of varying the length of the LRD section on the maximum tension reduction, in the parked load case, for two rated tensions. For each curve shape, one rated tension is set 0.5 MN below the 'optimal' rated tension defined in Section 3.2, the other is set 0.5 MN above.

For all stiffness curve shapes, increase in LRD length leads to higher reductions in maximum tension. The gains in tension reduction tend to be greater in the scenarios where the base-case mooring has little compliance (Fig. 14d). However, these benefits are regressive: once sufficient compliance is reached, increasing the length of the LRD has less effect on the tension reduction.

These trends also vary across the three curve shapes considered. In particular, for the 3-phase stiffness curves, varying the LRD lengths can change the optimal rated tension of the LRD. This has significant implications for LRD design: using shorter LRDs, which provide less compliance, requires higher rated tensions to avoid extending into the third-phase stiffness. Conversely, with longer LRDs, the lower rated tensions can provide greater tension reduction. This benefit is especially significant for the 3 MN TFI curve, which is operating in its stiff, third phase stiffness when the LRD is too short, thus not providing adequate compliance, but can provide much higher tension reduction when the length of the device is increased.

5.3. Influence of LRD length on maximum platform surge

The wind-induced surge (i.e. horizontal platform offset) increase introduced by LRDs, which constitutes additional 'quasi-static' platform offset along the axis of loading, is expected to be driven by the extension of the LRD (see Fig. 12). The extension of the LRD, as was shown in Fig. 15, is itself dependent on both its length and rated tension. Thus, to get a better idea of the effect of the LRD stiffness curves on surge, multiple combinations of lengths and rated tensions should be considered. Fig. 14 shows the effect of varying the length of the LRD section on the added surge, in the operational load case, for two rated tensions. For each curve shape, one rated tension is set 0.5 MN below the 'optimal' rated tension defined in Section 3.2, the other is set 0.5 MN above.

As expected, the increased length of LRDs leads to more surge of the operational turbine, across all 4 mooring scenarios. However, Fig. 15 also shows that the increased surge can be mitigated by using a stiffer LRD, i.e., with a higher rated tension. This is especially true for the 3-phase stiffness curves, where a 1 MN higher rated load can lead to over 60% reduction in additional surge. This is due to the slightly stiffer LRD not fully entering its second phase stiffness when in operation, and consequently extending much less, which can come at the cost of sightly lower tension reduction (see Fig. 14). For the three-phase stiffness curves, this trade off is not linear, and using the stiffer LRDs can be beneficial as it significantly reduces surge for only small increase in tension. For instance, in the taut 75 m depth case with a 20 m TFI device, using a 4 MN curve instead of 3 MN leads to 45% less surge increase (Fig. 15d), at the cost of only 5% less tension reduction benefit (Fig. 14d).

The underlying principle here is the coupling between variables: the rated tensions which provide optimal tension reduction for a 20 m LRD, as defined in Section 3.2, may not be optimal for other LRD lengths. Similarly, the LRD lengths which provide acceptable surge (i.e. horizontal platform offset) increase for a given rated tension and stiffness curve shape, may not be acceptable for other rated tensions. Hence, LRD design should be attempted holistically, where different combinations of LRD length, stiffness curve shape, and rated tension are assessed in parallel, to obtain the required reduction in fairlead tension which fits platform motion constraints.

6. Conclusion

The LRDs with 3-phase non-linear stiffness curves, featuring a high initial and final stiffness with a low-stiffness second phase, performed better than 'single-phase' curves both in terms of maximum tension and DEL reduction. This was true regardless of the water depth, mooring configuration, and load case. However, optimal tension reduction for 3-phase curves is highly dependent on finding the right rated tension, to ensure the LRD operates in the second phase of the curve. The single-phase stiffness curves were shown to offer similar tension reduction performance regardless of rated tension. In terms of platform motions,

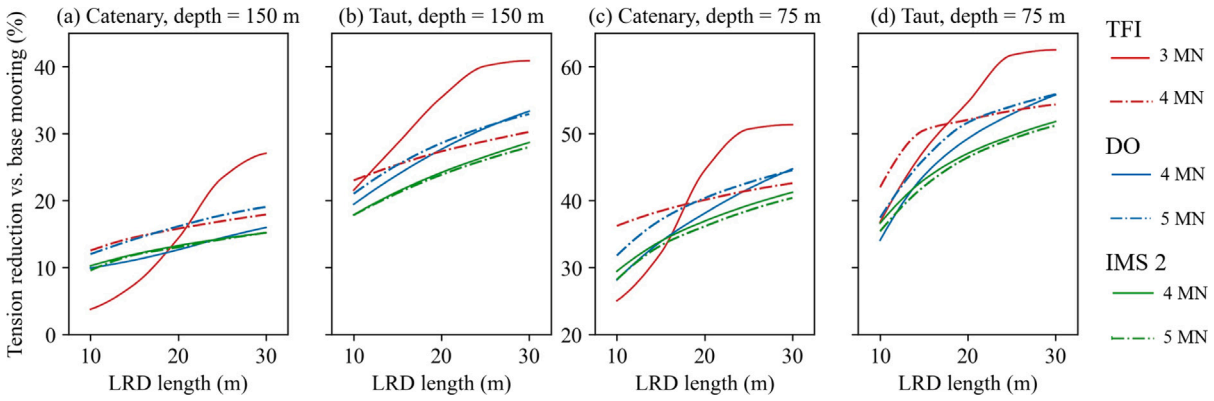

Fig. 14. Effect of varying the LRD length on maximum tension reduction compared to the base-case mooring, for the parked load case. Two rated tensions are considered, either side of the optimal rated tensions defined in Section 3.2.

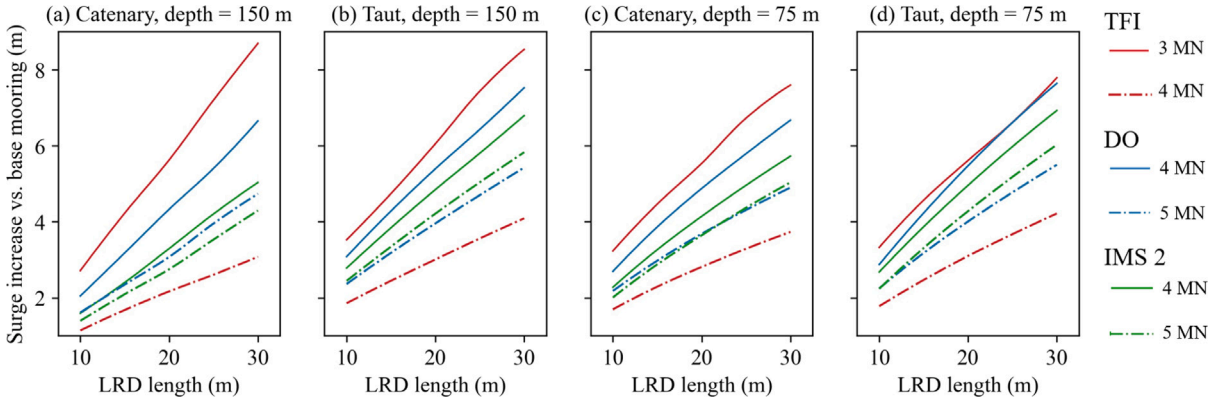

Fig. 15. Effect of varying the LRD length on surge increase (i.e. horizontal platform offset difference) compared to the base-case mooring, for the operational load case. Two rated tensions are considered, either side of the optimal rated tensions defined in Section 3.2.

all LRD curve shapes had similar effects on the system. Amplitudes of wave-induced surge (i.e. horizontal platform offset), heave, pitch and nacelle accelerations were reduced. Wind-induced surge was increased, especially in the operational load case, and was shown to be mainly affected by LRD length rather than curve shape.

Finding the optimal LRD design for a specific application involves determining the combination of rated tension and device length that provide suitable tension reduction whilst maintaining allowable platform surge. For 3-phase stiffness curves, there will typically be an interval of rated tensions that provide highest tension reduction. This interval is dependent on the length (or maximum extension) of the LRD, and thus must be determined with a multivariate analysis.

Two further conclusions can be drawn, valid across all LRD curves for the specific set of input conditions considered in this study: 1. LRDs provided more tension reduction in mooring systems with lower compliance, i.e. high modulus taut moorings, and shallower waters; and 2. LRDs provided more tension reduction in extreme parked conditions than extreme operational conditions. In future work, investigating a wider range of environmental conditions could be beneficial, to further assess how the LRD's performance and optimal design parameters vary depending on the expected wave height and wind speed.

CRediT authorship contribution statement

Oscar Festa: Writing – original draft, Visualization, Validation, Software, Methodology, Formal analysis, Conceptualization. **Susan Gourvenec:** Writing – review & editing, Supervision, Resources, Methodology, Funding acquisition, Conceptualization. **Adam Sobey:** Writing – review & editing, Resources, Conceptualization.

Declaration of competing interest

The authors declare that they have no known competing financial interests or personal relationships that could have appeared to influence the work reported in this paper.

Data availability

Data will be made available on request.

Acknowledgments

This work forms part of the activities of the Royal Academy of Engineering Chair in Emerging Technologies Centre of Excellence for Intelligent & Resilient Ocean Engineering (www.southampton.ac.uk/iroe), based at the University of Southampton. Susan Gourvenec is supported by the Royal Academy of Engineering, UK under the Chairs in Emerging Technologies scheme. Adam Sobey is supported by the Lloyd's Register Foundation, UK. The authors thank Aengus Connolly for his advice on Flexcom.

Appendix. Stiffness of full mooring systems

The stiffness of a full mooring system, including all of its components (in this case, LRD and rope or chain) is defined as the relationship between the position of the platform and the subsequent restoring force imparted on the platform (i.e. fairlead tension). The mooring stiffness dictates the equilibrium position of the platform for a given mean load,

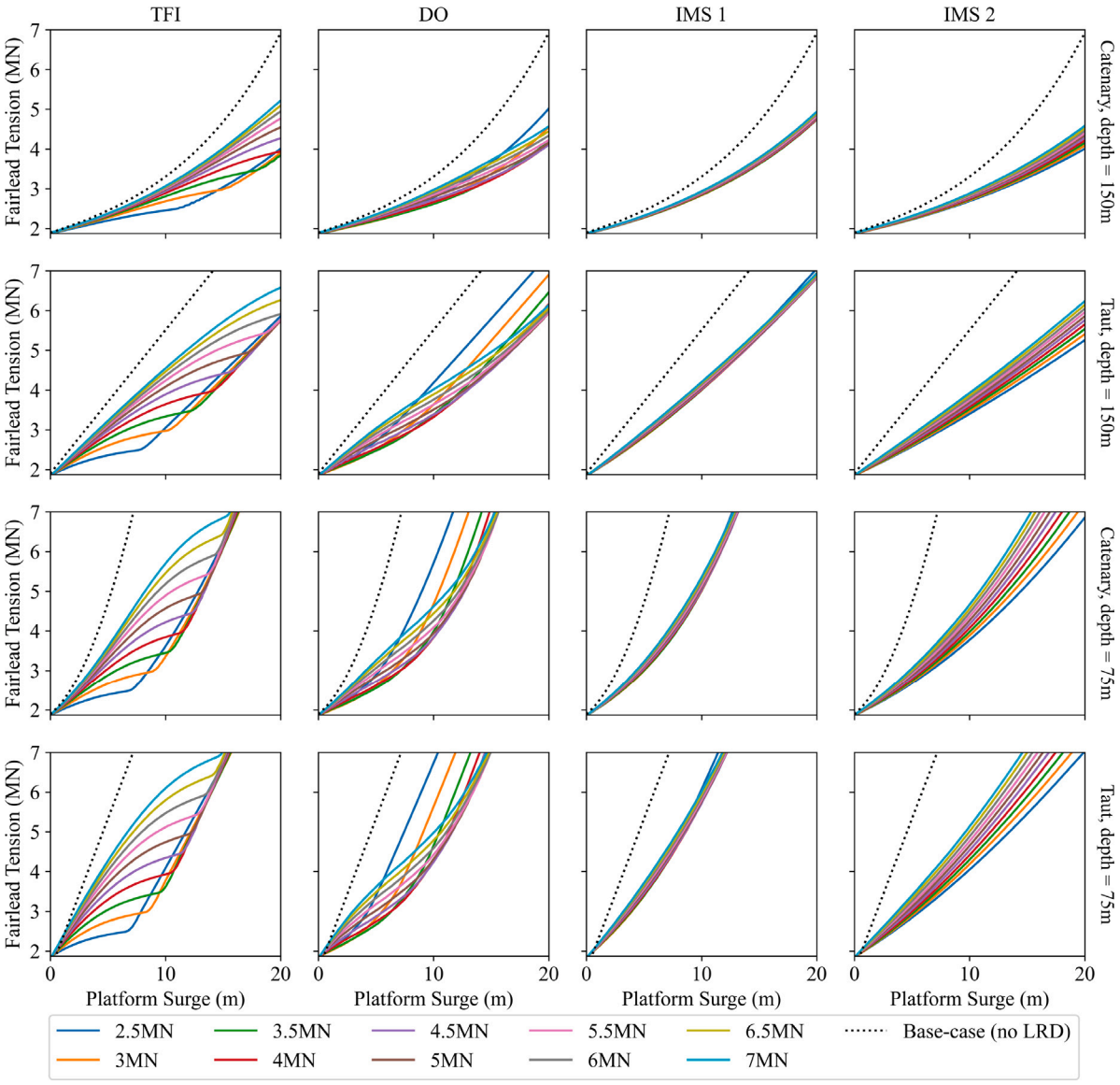

Fig. A.1. Stiffness curves of the full mooring system (i.e., mooring line + LRD) for all combinations of mooring scenarios, LRD curve shapes, and LRD rated tensions.

and the slope of the stiffness curve about this mean load then affects the dynamic response of the mooring.

The full mooring system stiffness is highly dependent on the stiffness of the LRD, but is also driven by the response of the catenary chain or taut rope which forms the rest of the mooring line. To obtain the stiffness profile of the full system, the platform was slowly displaced along the surge axis, and the fairlead tension required for static equilibrium was calculated at every step. Resulting plots of fairlead tension against surge (i.e. horizontal platform offset) are shown in Fig. A.1. These plots illustrate some useful concepts:

- The shallower and taut mooring systems exhibit higher stiffness, which translates to lower surge (i.e. horizontal platform offset) for the same value of fairlead tension.
- The taut moorings are generally less compliant than the catenary mooring, and their stiffness is more dominated by the stiffness of the LRD. In other words, the stiffness curve of the taut mooring system is very similar to that of the LRD, as the rope does not contribute much to the compliance.
- In the case of a 3-phase LRD stiffness curve (TFI, DO), low rated tensions can actually lead to much stiffer mooring systems once a certain value of surge is reached, as the LRD compliance is rapidly exhausted, leading to operation in the stiff, third-phase of the curve.

References

Allen, C., Viscelli, A., Dagher, H., Goupee, A., Gaertner, E., Abbas, N., Hall, M., Barter, G., 2020. Definition of the UMaine volturnUS-S reference platform developed for the IEA wind 15-megawatt offshore reference wind turbine. http://dx.doi.org/10.2172/1660012, URL: https://www.osti.gov/biblio/1660012.

ASTM International, 2011. Standard practice for cycle counting in fatigue analysis. ASTM E1049-85.

Bach-Gansmo, M., Garvik, S., Thomsen, J., Andersen, M., 2020. Parametric study of a taut compliant mooring system for a FOWT compared to a catenary mooring. J. Mar. Sci. Eng. 8, http://dx.doi.org/10.3390/jmse8060431.

Brydon, 2022. Moorline polyester [Datasheet]. URL: https://www.brydon.com/products/moorline-polyester.

Dublin Offshore, 2020. Load reduction device (LRD) – how it works. URL: https://www.dublinoffshore.ie/media/pages/technology/6f4e7419f6-1635594571/how-it-works.pdf.

Festa, O., Gourvenec, S., Sobey, A., 2022. Proxy model for the design of extensible floating offshore wind turbine mooring systems. In: International Ocean and Polar Engineering Conference. URL: https://eprints.soton.ac.uk/457472/1/2022_Festa_et_al_ISOPE.pdf.

Festa, O., Gourvenec, S., Sobey, A., 2023. Analytical model of non-linear load reduction devices for catenary moorings. In: International Conference on Offshore Mechanics and Arctic Engineering. URL: https://eprints.soton.ac.uk/457472/1/2022_Festa_et_al_ISOPE.pdf.

FLEXCOM, 2022. Flexcom comparison to FAST results for 15 MW Volturn-US FOWT. URL: https://flexcom.fea.solutions/l04---umaine-volturnus-s-iea15.html.

Fontaine, E., Kilner, A., Carra, C., Washington, D., Ma, K., Phadke, A., Laskowski, D., Kusinski, G., 2014. Industry survey of past failures, pre-emptive replacements and reported degradations for mooring systems of floating production units. In: OTC Offshore Technology Conference. http://dx.doi.org/10.4043/25273-MS, arXiv:https://onepetro.org/OTCONF/proceedings-pdf/14OTC/4-14OTC/D041S047R002/1505598/otc-25273-ms.pdf.

Gaertner, E., Rinker, J., Sethuraman, L., Zahle, F., Anderson, B., Barter, G., Abbas, N., Meng, F., Bortolotti, P., Skrzypinski, W., Scott, G., Feil, R., Bredmose, H., Shields, M., Dykes, K., Allen, C., Viselli, A., 2020. IEA wind TCP task 37: Definition of the IEA 15-megawatt offshore reference wind turbine. http://dx.doi.org/10.2172/1603478, URL: https://www.osti.gov/biblio/1603478.

Harrold, M., Thies, P., Newsam, D., Ferreira, C., Johanning, L., 2020. Large-scale testing of a hydraulic non-linear mooring system for floating offshore wind turbines. Ocean Eng. 206, 107386. http://dx.doi.org/10.1016/j.oceaneng.2020.107386, URL: https://www.sciencedirect.com/science/article/pii/S0029801820304145.

International Electrotechnical Commission, 2019. IEC 61400-3:2019 - Wind energy generation systems - Part 3: Design requirements for offshore wind turbines. URL: https://www.iso.org/standard/72447.html. (Accessed 24 March 2023).

Khalid, F., Johanning, L., Thies, P., Newsam, D., 2020. Assessment of Potential Sites for a Non-Linear Mooring System in Floating Offshore Wind Applications. pp. 650–656. http://dx.doi.org/10.1201/9781003134572-74.

Lozon, E., Hall, M., McEvoy, P., Kim, S., Ling, B., 2022. Design and analysis of a floating-wind shallow-water mooring system featuring polymer springs. In: International Offshore Wind Technical Conference. Vol. 486.

Luxmoore, J., Grey, S., Newsam, D., Johanning, L., 2016. Analytical performance assessment of a novel active mooring system for load reduction in marine energy converters. Ocean Eng. 124, 215–225. http://dx.doi.org/10.1016/j.oceaneng.2016.07.047, URL: https://www.sciencedirect.com/science/article/pii/S0029801816302955.

Ma, K., Luo, Y., Kwan, T., Wu, Y., 2019. Chapter 4 - Mooring design. In: Mooring System Engineering for Offshore Structures. Gulf Professional Publishing, pp. 63–83. http://dx.doi.org/10.1016/B978-0-12-818551-3.00004-1.

Ma, K., Wu, Y., Stolen, S.F., Bello, L., ver der Horst, M., Luo, Y., 2021. Mooring designs for floating offshore wind turbines leveraging experience from the oil & gas industry. In: International Conference on Offshore Mechanics and Arctic Engineering. Vol. 1, http://dx.doi.org/10.1115/OMAE2021-60739.

McEvoy, P., Johnston, E., 2019. Polymer mooring component for offshore renewable energy. In: OTC Offshore Technology Conference. http://dx.doi.org/10.4043/29587-MS.

McEvoy, P., Kim, S., 2017. Mooring load management for SR2000 floating tidal device using non-linear polymer components. In: 12th European Wave and Tidal Energy Conference. URL: https://uploads-ssl.webflow.com/5f8964a5a533790d6cc8820a/5f96cb7a8ba32845a778cb9e_EWTEC-2017.pdf.

McEvoy, P., Kim, S., Haynes, M., 2021. Fibre spring mooring solution for mooring floating offshore wind turbines in shallow water. In: International Conference on Offshore Mechanics and Arctic Engineering. http://dx.doi.org/10.1115/OMAE2021-62892, V009T09A029.

Offshore-mag.com, 2021. Floating wind load suppression system completes prototype trials. URL: https://www.offshore-mag.com/renewable-energy/article/14205082/floating-wind-load-suppression-system-completes-prototype-trials.

OffshoreWind.biz, 2021. EMEC verifies Dublin Offshore's floating wind mooring component. URL: https://www.offshorewind.biz/2021/03/12/emec-verifies-dublin-offshores-floating-wind-mooring-component/.

Pillai, A., Gordelier, T., Thies, P., Cuthill, D., Johanning, L., 2022. Anchor loads for shallow water mooring of a 15 MW floating wind turbine—Part II: Synthetic and novel mooring systems. Ocean Eng. 266, 112619. http://dx.doi.org/10.1016/j.oceaneng.2022.112619, URL: https://www.sciencedirect.com/science/article/pii/S0029801822019023.

Robertson, A., Gueydon, S., Bachynski-Polić, E., Wang, L., Jonkman, J., Alarcon Fernandez, D., Amet, E., Beardsell, A., Bonnet, P., Boudet, B., Brun, C., Chen, Z., Féron, M., Forbush, D., Galinos, C., Galvan, J., Gilbert, P., Gómez, J., Harnois, V., Wohlfahrt-Laymann, S., 2020. OC6 Phase I: Investigating the underprediction of low-frequency hydrodynamic loads and responses of a floating wind turbine. J. Phys. Conf. Ser. 1618, 032033. http://dx.doi.org/10.1088/1742-6596/1618/3/032033.

Taboada, M., Ortega, A., Martín, R., Pombo, A., Moreu, J., 2020. An evaluation of the effect that motions at the nacelle have on the cost of floating offshore wind turbines. In: OTC Offshore Technology Conference. http://dx.doi.org/10.4043/30632-MS.

WindEurope, 2017. Floating offshore wind vision statement. URL: https://windeurope.org/wp-content/uploads/files/policy/position-papers/Floating-offshore-wind-energy-a-policy-blueprint-for-Europe.pdf.

Xu, K., Larsen, K., Shao, Y., Zhang, M., Gao, Z., Moan, T., 2020. Design and comparative analysis of alternative mooring systems for floating wind turbines in shallow water with emphasis on ultimate limit state design. Ocean Eng. 219, http://dx.doi.org/10.1016/j.oceaneng.2020.108377, URL: https://www.sciencedirect.com/science/article/pii/S0029801820312841.